

1 Grain-size-dependent remanence anisotropy and its implications for paleodirections and
2 paleointensities – proposing a new approach to anisotropy corrections

3

4 Andrea R. Biedermann¹, Dario Bilardello¹, Mike Jackson¹, Lisa Tauxe², Joshua M. Feinberg¹

5 ¹ Institute for Rock Magnetism, University of Minnesota, 116 Church St SE, Minneapolis, MN
6 55455, USA

7 ² Scripps Institution of Oceanography, University of California, San Diego, La Jolla, CA, USA

8

9

10 **Corresponding author**

11 Andrea R. Biedermann
12 237 John T Tate Hall
13 Institute for Rock Magnetism
14 University of Minnesota
15 116 Church St SE
16 Minneapolis, MN 55455
17 United States of America

18

19 andrea.regina.biedermann@gmail.com

20 +1 612 434 66 60

21

22

23 The final version of this article is available at the EPSL website,
24 <https://www.sciencedirect.com/science/article/pii/S0012821X19300834?dgcid=author>

25

26

27 **Keywords**

28 paleomagnetism; remanence anisotropy; anisotropy correction; paleodirection; paleointensity; Bushveld
29 Complex

30 Abstract

31 Paleomagnetic data provide information on the evolution of the Earth's magnetic field, and are used to
32 reconstruct plate motions. One fundamental assumption underlying these interpretations is that the
33 magnetization of a rock reliably records the direction and intensity of the magnetizing field, i.e. that the
34 magnetization is parallel to the field direction, and the intensity of magnetization is proportional to the
35 field strength. Preferred alignment or anisotropic distribution of magnetic grains can affect both the
36 direction and the intensity of magnetization. Therefore, correction techniques, employing the
37 anisotropy of magnetic susceptibility (AMS), thermal remanence (ATRM), or anhysteretic remanence
38 (AARM) are used to account for these effects. We find that AARM within the same rock can vary
39 dramatically with coercivity/grain size, so that anisotropy corrections can also depend on how AARM
40 was measured.

41 A consequence of the dependence of AARM on coercivity is that although a specimen may have been
42 magnetized in a single direction, different grain size fractions may record magnetizations in different
43 orientations. These directional variations, as revealed during progressive alternating field (AF)
44 demagnetization, could erroneously be interpreted as changes in field or reorientation of the rock unit,
45 when in reality they are related to grain-size-dependent remanence anisotropy. Similarly, intensity
46 variations caused by grain-size-dependent anisotropy may bias paleointensity estimates. These
47 observations have important consequences for studies on the evolution of the Earth's magnetic field,
48 magnetic overprinting, and paleogeographic reconstructions.

49 1. Introduction

50 Reliable paleomagnetic data, i.e. paleomagnetic directions and paleointensities, are essential for (1)
51 describing the past evolution of the Earth's magnetic field which in turn helps understand the
52 geodynamo and forms the basis for archeomagnetic dating, and (2) for paleogeographic reconstructions.
53 Paleointensity data are used to characterize the processes related to magnetic field reversals or the
54 absence of such reversals (superchrons), and paleosecular variation (Biggin et al., 2012; Prévot et al.,
55 1985; Tarduno et al., 2006; Tauxe and Yamazaki, 2015), date archeological materials (Ben-Yosef et al.,
56 2010; Stillinger et al., 2016), estimate the onset of inner core growth (Biggin et al., 2015; Buffett, 2003;
57 Hale, 1987; Tarduno et al., 2006), or determine whether extraterrestrial bodies also possess
58 geodynamos (Cisowski et al., 1983). Directional data provide information for paleogeographic
59 reconstructions of plate configurations (Dietz and Holden, 1970; Hospers and van Andel, 1969; Irving,
60 1957; Morel and Irving, 1981), and help evaluate the symmetry and dipole- versus non-dipole
61 components of the field (Evans, 1976; Pesonen and Nevanlinna, 1981; Swanson-Hysell et al., 2009;
62 Tauxe and Kent, 2004; van der Voo and Torsvik, 2001).

63 Two fundamental assumptions in paleomagnetic and paleointensity studies are that (1) the
64 magnetization is parallel to the inducing field, and (2) the intensity of the magnetization is proportional
65 to the field. Some of the challenges in obtaining and interpreting paleomagnetic data include the non-
66 continuity of the record, alteration and remagnetization of rocks (Dunlop et al., 1997; Elmore et al.,
67 2012), limited stability of magnetic grains (Levi, 1977), cooling rate effects (Bowles et al., 2005; Walton,
68 1980; Yu, 2011), a non-linear relationship between field strength and thermal remanence (Coe, 1967;
69 Selkin et al., 2007), low-field bias in paleointensity data (Smirnov et al., 2017) and anisotropy (Rogers et
70 al., 1979; Kent and Irving, 2010; Selkin et al., 2000). Paleomagnetic studies on magnetic inclusions within

71 silicates have been successful in overcoming some of these issues, because these magnetic inclusions
72 are protected against alteration by their host silicates, and because they are confined to a certain size
73 range (Cottrell and Tarduno, 1999; Feinberg et al., 2005; Tarduno et al., 2006; Selkin et al., 2008).
74 However, one potential problem with such inclusions is that they generally have a preferred orientation
75 with respect to the silicate lattice, resulting in anisotropic remanence acquisition if the silicates are
76 aligned (Feinberg et al., 2006).

77 Anisotropy affects both the direction and intensity of magnetization, with important consequences for
78 inferred apparent polar wander paths, paleogeographic reconstructions, or paleointensity studies. The
79 simplest way to correct for these effects is by measuring anisotropy of magnetic susceptibility (AMS) and
80 multiplying the observed magnetization vector with the inverse of the AMS tensor, i.e. because $\vec{M} = k * \vec{H}$,
81 it follows that $\vec{H} = inv(k) * \vec{M}$. However, AMS is usually unrepresentative of remanence anisotropy,
82 and has been described as inadequate for detecting paleofield deflections in paleomagnetism (Selkin et
83 al., 2000), archeomagnetism (Borradaile et al., 2001; Tema, 2009), and extraterrestrial magnetism
84 (Gattacceca et al., 2003). Anisotropy of thermal, anhysteretic, or isothermal remanent magnetization
85 (ATRM, AARM, and AIRM) are more direct representations of the anisotropy of remanence carrying
86 grains. Because of possible alteration during thermal experiments, AARM is often preferred to assess
87 remanence anisotropy (Potter, 2004), and Mitra et al. (2013) demonstrated that AARM and ATRM
88 corrections can give comparable results for some specimens. But, care has to be taken when the
89 remanence is carried by grains other than single domain magnetite for which Néel theory applies,
90 because coercivities cannot be easily related directly to blocking temperatures. If several different
91 minerals contribute to the NRM or the remanence anisotropy, the magnetization of each mineral needs
92 to be corrected with its own specific anisotropy (Borradaile and Almqvist, 2008; Kodama and Dekkers,
93 2004). Similarly, if subpopulations of the same mineral but different grain sizes possess different
94 anisotropies, one would expect that the remanence carried by each subpopulation would be affected by
95 its own anisotropy. It has been demonstrated that the preferred alignment of distinct sub-populations of
96 magnetite grains can be characterized by measuring the anisotropy of partial ARMs (ApARMs) (Jackson
97 et al., 1988). A number of studies have since used ApARMs to capture the remanence anisotropies of
98 specific grain sizes to describe primary vs secondary fabrics, or differences in fabrics recorded by
99 different grain sizes (Aubourg and Robion, 2002; Bilardello and Jackson, 2014; Trindade et al., 1999).
100 Even though these studies illustrate that ApARMs in the same rock can vary dramatically with grain size
101 or coercivity window, most studies still measure AARMs by imparting a remanence in the 0-100 mT AF
102 range, thus measuring an averaged anisotropy over all the coercivity windows in the specimen.

103 Remanence anisotropy varies with coercivity in a large variety of specimens with multiple remanence
104 carriers. This calls for a more complete assessment of how changes in remanence anisotropy with grain
105 size affect magnetization direction and intensity, and relevant implications for anisotropy corrections. In
106 this study, we measured a series of ApARM and the analogous anisotropy of partial TRMs (ApTRM)
107 tensors. While ApTRM experiments have been inconclusive, we will show how ApARM tensors within
108 the same specimen can change among low, intermediate and high coercivity windows, and how these
109 ApARM tensors compare to the AARM tensors measured over typical coercivity ranges used in AARM
110 experiments. Each of these A(p)ARM tensors can be used to predict how much the intensity and
111 direction of the magnetization would differ from that observed in an isotropic specimen for any given
112 field direction. These predictions represent the expected uncertainty in paleodirection and
113 paleointensity estimates, and how these vary with the coercivity fraction of the remanence-carrying

114 grains. To illustrate how grain-size-dependent remanence anisotropy may affect NRM acquisition, we
115 investigate the direction of an ARM imparted along the specimen z-axis (randomly oriented with
116 respect to the anisotropy principal axes), with a special focus on changes in magnetization direction
117 during AF demagnetization and acquisition of an ARM. This experiment underlines how for a given field
118 direction, the magnetization direction in the same specimen can change according to variations in the
119 AARM tensor with coercivity/grain size.

120 Based on these investigations, we develop a conceptual model for anisotropic remanence acquisition in
121 rocks with complex fabrics, and propose a new procedure for anisotropy corrections. In particular, we
122 suggest that (1) ApARMs are measured for different coercivity windows, (2) the ApARM determined in
123 the coercivity window that carries the characteristic remanence is used for anisotropy corrections, and
124 (3) the directional data of ARM demagnetization or ARM acquisition experiments is also processed, in
125 order to provide a first measure of how strongly remanence anisotropy varies with grain size.

126 2. Materials

127 Specimens used in this study are gabbronorites from the Bushveld Complex, South Africa, with preferred
128 orientation of pyroxene, plagioclase, and remanence-carrying grains within these silicates (Feinberg et
129 al., 2006). Several existing paleomagnetic studies on rocks from the Bushveld Complex report paleopoles
130 with considerable spread, which has been attributed to differences in emplacement ages and/or post-
131 emplacement deformation related to re-equilibration of isostasy (Hattingh, 1986; Letts et al., 2009, and
132 references therein). Because anisotropy affects magnetization directions and neither of these studies
133 corrected for these effects, anisotropic remanence acquisition could be another possible explanation. In
134 this study, we have measured ApARMs and AARMs on eight specimens, followed by A(p)TRM
135 measurements on a subset of four of these, and compared the new results to directional data from
136 previous paleointensity experiments on 35 of the Bushveld specimens.

137 3. Methods

138 3.1 Paleointensity

139 Paleointensity experiments followed the IZZI-Thellier protocol (Yu et al., 2004). The specimens were
140 thermally demagnetized in a laboratory-built, non-inductively wound furnace whose temperature is
141 monitored via three thermocouples and is controlled through a LabView module at the Scripps
142 Institution of Oceanography, UC San Diego, at temperatures up to 550 °C. Partial thermal remanences
143 (pTRMs) were imparted parallel to the specimen z-axes in a field of 20 μ T during cooling. For this study,
144 we were mainly interested in the direction of the imposed pTRM at every temperature step. This
145 magnetization was calculated as a vector difference between the demagnetized and the magnetized
146 states for the same temperature.

147 3.2 Remanence anisotropy

148 TRM and pTRM anisotropies were characterized by applying a 50 μ T field while specimens were cooling
149 from 600°C to room temperature in an ASC-Scientific TD48SC furnace. Subsequently, all specimens
150 were demagnetized to 500°C, then to 550°C, in order to determine the ApTRM₅₀₀₋₆₀₀ and ApTRM₅₅₀₋₆₀₀.
151 After each step, TRMs were measured on a 2G Enterprises 760-R SQUID superconducting rock
152 magnetometer (SRM). This procedure was repeated for three directions (x, y and z) on a thermally
153 demagnetized specimen, followed by a full TRM along the x-axis, in order to check for specimen

154 alteration. The difference between the first and second measurement of the full TRM parallel to x
155 should be distinctly smaller than the differences between the full TRMs acquired parallel to the x, y, and
156 z axes that are related to anisotropy. TRM anisotropy tensors were calculated from the full-vector
157 magnetizations.

158 A series of seven ApARM/AARM tensors was determined for each specimen, using coercivity windows of
159 0-20, 20-50, 50-100, 100-180, and 0-50, 0-100, 0-180 mT. The former series will be referred to as
160 ApARMs (e.g., ApARM₂₀₋₅₀), and the latter as AARMs (e.g., AARM₀₋₅₀) throughout this paper. For each
161 dataset, a 0.1 mT DC field was applied on a DTech D-2000 AF demagnetizer in the respective AF
162 demagnetization interval. Decay rates varied from 0.0001 mT/half-cycle for AF ≤ 5 mT, to 0.0075
163 mT/half-cycle at 200 mT AF. The remanence was subsequently measured on the 2G-760 SRM. The
164 procedure was repeated for 9 orientations, and specimens were demagnetized to 200 mT AF in-
165 between steps. ApARM and AARM remanence susceptibility tensors were then computed using the
166 field-parallel remanence components, $M_{||} = \vec{M} \cdot \mathbf{k}\vec{H}/|\vec{H}|$, analogous to the conventional method for
167 AMS calculation.

168 All remanence anisotropy tensors are characterized by their eigenvalues ($k_1 \geq k_2 \geq k_3$) and
169 eigenvectors, the mean (p)ARM or (p)TRM $k_{mean} = (k_1 + k_2 + k_3)/3$, the anisotropy degree $P =$
170 k_1/k_3 or $k' = \sqrt{((k_1 - k_{mean})^2 + (k_2 - k_{mean})^2 + (k_3 - k_{mean})^2)/3}$, and the shape $U =$
171 $(2 * k_2 - k_1 - k_3)/(k_1 - k_3)$. U varies from -1 for rotationally prolate ellipsoids to +1 for rotationally
172 oblate ones, and we will use the terms 'oblate' and 'prolate' to describe fabrics with $0 < U < 1$ and $-1 < U$
173 < 0 , respectively. Hext (1963) statistics, i.e. confidence ellipses and F-tests, was used to determine
174 whether a specimen possesses a significant anisotropy in each coercivity or temperature window, and
175 whether principal directions of different windows are distinct at the 95% confidence level.

176 3.3 Effects of magnetic anisotropy on remanence acquisition

177 To investigate the anisotropy-related NRM deflections and intensity variations including their
178 dependence on coercivity, the magnetization vector, $\vec{M} = \mathbf{k}\vec{H}$ was compared to the intensity of
179 magnetization, $M = k_{mean}H$, and the direction of the inducing field, \vec{H} . For each ApARM and AARM
180 tensor, the expected angular deviations were computed for all possible field orientations as the acute
181 angle between \vec{M} and \vec{H} , and the corresponding intensity deviations by $|\vec{M}|/M$.

182 Finally, specimens were given an ARM parallel to the specimen z-axis in a 0.1 mT DC field applied over 0-
183 200 mT AF. This ARM, imparted to represent an NRM acquired in a constant field, was subsequently
184 stepwise AF demagnetized (steps of 2, 5, 10, 15, 20, 30, 40, 50, 60, 70, 80, 90, 100, 120, 140, 160, 180,
185 200 mT). Intensity and direction of the remaining remanence were measured after each
186 demagnetization step. After demagnetization to 200 mT, a new ARM, again parallel to z, was stepwise
187 imposed on the specimen using the same steps as for the demagnetization, again measuring the
188 remanence direction as well as intensity after each step. The resulting remanence direction during AF
189 demagnetization and ARM acquisition was then compared to the known field direction. The field
190 intensity, calculated from the magnetization and A(p)ARM tensors was compared to the known intensity
191 of the applied DC field. Because this experiment is prone to uncertainties caused by slight changes in
192 specimen orientation each time the specimen is inserted in the magnetometer, the same experiment
193 was repeated on a 2G model 755 SRM with an in-line ARM/AF system. With this setup, specimens
194 remained untouched during the entire AF demagnetization or acquisition of ARM. Because the in-line

195 system can only reach 170 mT, the steps for these experiments were 2, 5, 10, 15, 20, 30, 40, 50, 60, 70,
196 80, 90, 100, 120, 140, 160, 170 mT. Note that the decay rates for the in-line ARM/AF system are related
197 to the speed at which specimens move (15 cm/s) and are thus different for each field. Note that the
198 arbitrary choice of field orientation means that the ARM direction may be close to a principal axis of one
199 or all the ApARM tensors, resulting in little or no deflection even in anisotropic specimens. Hence, this
200 experiment is an easy way to show that anisotropy is present if a deflection is detected. However, it
201 cannot be used to rule out the presence of anisotropy entirely if no deflection is observed.

202 4. Results

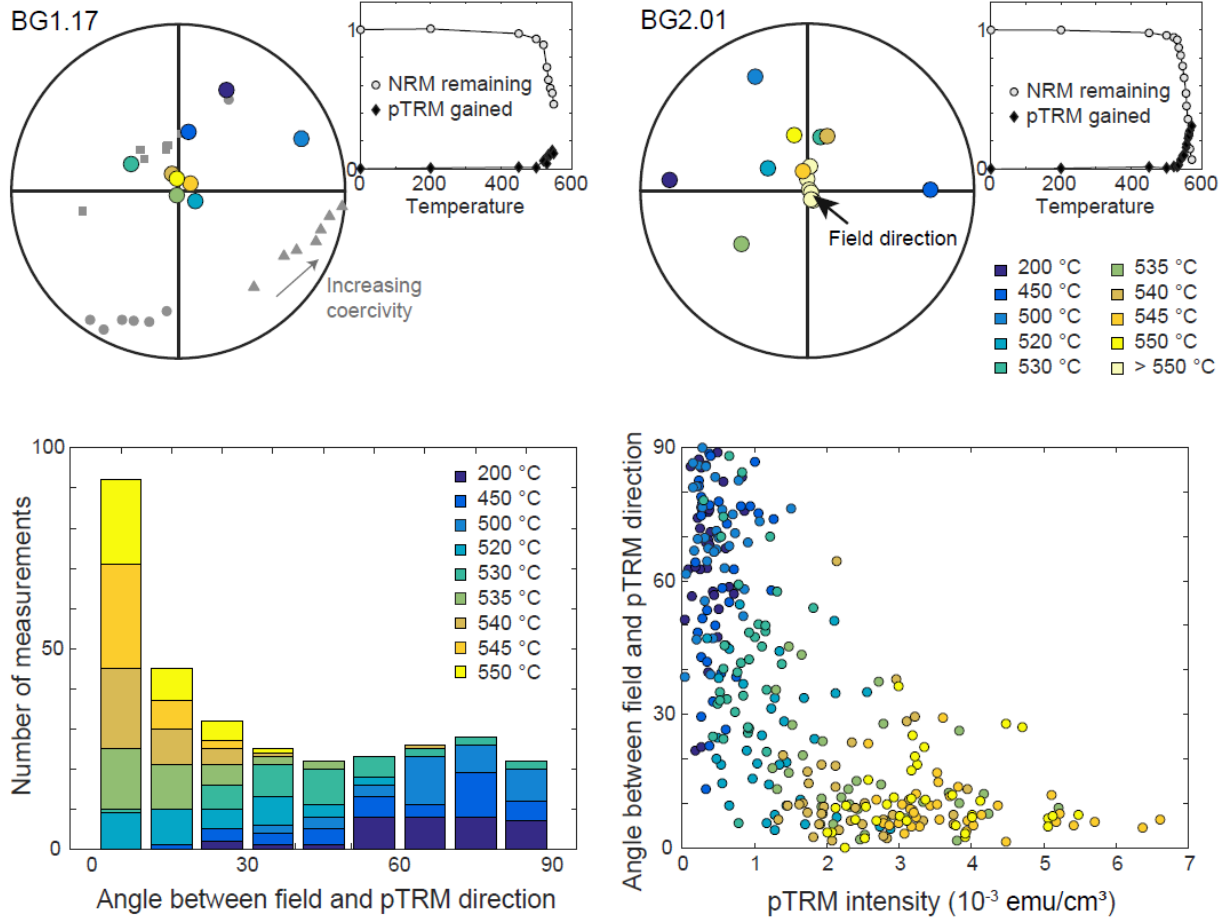
203 4.1 Directions of pTRMs acquired during paleointensity experiments

204 The directions of pTRMs acquired during the paleointensity experiments are dispersed around the field
205 direction. The angle between magnetization and field orientations is generally larger at lower
206 temperatures than at higher temperatures, ranging from sub-parallel to the applied field to nearly
207 perpendicular to the field. In addition, there appears to be a systematic deflection away from the
208 laboratory field at most temperatures for some of the specimens (Figure 1).

209 4.2 TRM anisotropy

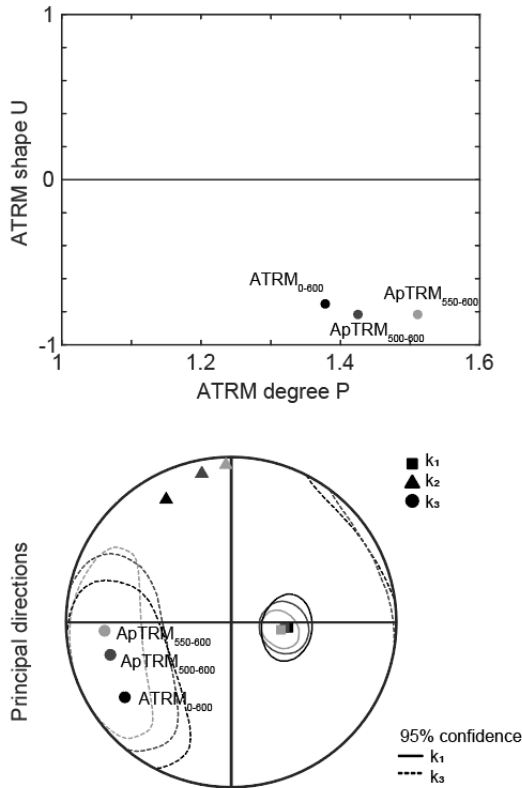
210 Three out of four specimens show differences between the first and second set of TRMs acquired
211 parallel to x. The difference, defined by $\Delta M_x = (M_{x,alteration\ check} - M_{x,initial})/M_{x,initial}$, are between
212 -5.6 and +15.8%. In addition, it appears that the TRM acquired along one direction does not fully
213 remagnetize when applying a perpendicular TRM. From these two observations we conclude that (1)
214 specimens may have chemically altered during the experiment, and/or (2) the Thellier Laws of
215 reciprocity and independence do not hold for these specimens. For one specimen, BG2.09a, ΔM_x equals
216 -0.2%. This is the only specimen for which (p)TRM anisotropy will be reported (Table A, online
217 supplementary). Figure 2 shows that the maximum ATRM axes of all three tensors coincide. There
218 seems to be a rotation of the minimum and intermediate axes from ATRM₀₋₆₀₀ to ApTRM₅₀₀₋₆₀₀ to
219 ApTRM₅₅₀₋₆₀₀; however, this change in direction is not statistically significant due to the large e_{23}
220 confidence angle. The degree of anisotropy increases with increasing lower temperature of the ApTRM
221 window.

222



223

224 *Figure 1: (top) Stereoplots showing directions of pTRMs for two specimens acquired during*
 225 *paleointensity experiments; colors indicate temperature. Insets show NRM remaining and pTRM gained*
 226 *for each specimen, with all magnetizations normalized to the initial NRM. For BG1.17, A(p)ARM*
 227 *principal-axis orientations of sister specimen BG1.17a are also shown (grey circles, triangles and squares*
 228 *respectively for minimum, intermediate and maximum axes). (bottom) Histogram shows pTRM angular*
 229 *deflections (10° bins) for 35 specimens measured at 9 temperatures each.*



230

231 *Figure 2: Anisotropy degree P , shape U and principal directions for the three $A(p)$ TRM tensors of*
 232 *specimen BG2.09a. Note that the directions are not well defined, so that the apparent rotation of*
 233 *minimum and intermediate principal axes with temperature is not significant.*

234

235 4.3 ApARM and AARM tensors and effect on remanence direction and intensity

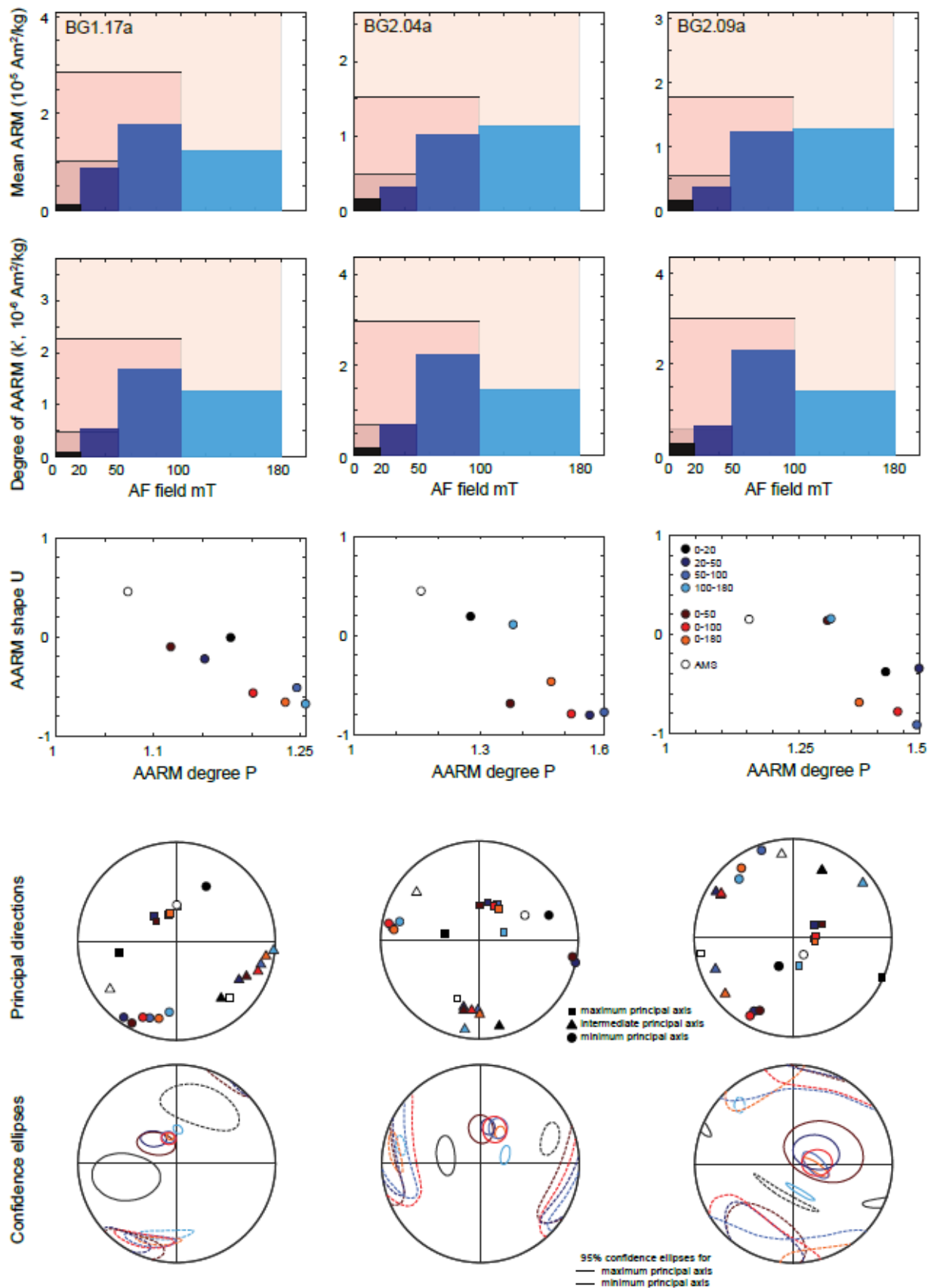
236 All specimens acquire ARMs, and these are generally anisotropic (Online Supplementary Tables B
 237 (summary) and C (all data)). Three specimens do not display significant anisotropy in the 0-20 mT AF
 238 window, where the mean ARM is lowest, and three samples have insignificant anisotropy in the 0-50 mT
 239 AF window, as defined by e_{13} confidence angles $> 26^\circ$ and $F > 9.01$ (Hext, 1963). For those tensors with
 240 significant AARM, the anisotropy degrees k' and P vary between $1.07 \cdot 10^{-7} \text{m}^3/\text{kg} - 4.64 \cdot 10^{-6} \text{m}^3/\text{kg}$, and
 241 $1.12 - 1.59$, respectively. For some ApARMs and AARMs in some specimens, the k_2 and k_3 values cannot
 242 be distinguished at 95% confidence, as indicated by $F_{23} < 9.55$ and large e_{23} confidence angles. The shape
 243 of the ARM anisotropy varies from $U = -0.92$ to $U = 0.46$. Figure 3 shows the mean ARM, anisotropy
 244 parameters and principal directions for each of the ApARM and AARM tensors for three representative
 245 specimens. The ApARM₀₋₂₀ has the weakest mean ARM, and also the weakest k' . Compared to the other
 246 ApARMs, ApARM₅₀₋₁₀₀ has the highest k' , which also dominates the combined AARMs, AARM₀₋₁₀₀ and
 247 AARM₀₋₁₈₀. The mean ARM, on the other hand, can be higher for AARM₁₀₀₋₁₈₀ than for AARM₅₀₋₁₀₀. These
 248 observations indicate that although the grains in the higher coercivity window possess higher overall
 249 remanence, owing to concentration and/or spontaneous magnetization, they have lower anisotropy
 250 than those in the 50-100 mT window.

251 The principal axes of several or all A(p)ARM tensors in the same specimen can have similar orientations;
252 however, they can also be dramatically different. In particular, the orientation of principal axes can be
253 significantly different for AARM₀₋₂₀ as compared to any of the other ApARMs or AARMs, i.e. the 95%
254 confidence ellipses do not overlap. The other ApARMs and AARMs show similar maximum principal axes
255 directions (overlapping confidence ellipses), however, the intermediate and minimum principal axes
256 appear to rotate with increasing coercivity (non-overlapping confidence ellipses). These differences in
257 principal axes orientations and degree and shape of anisotropy will result in different remanence
258 deflections and intensity changes for the grain populations in each of the coercivity windows, as defined
259 by their AARM and ApARM tensors (Figure 4).

260 4.4 Remanence direction for ARM parallel to z

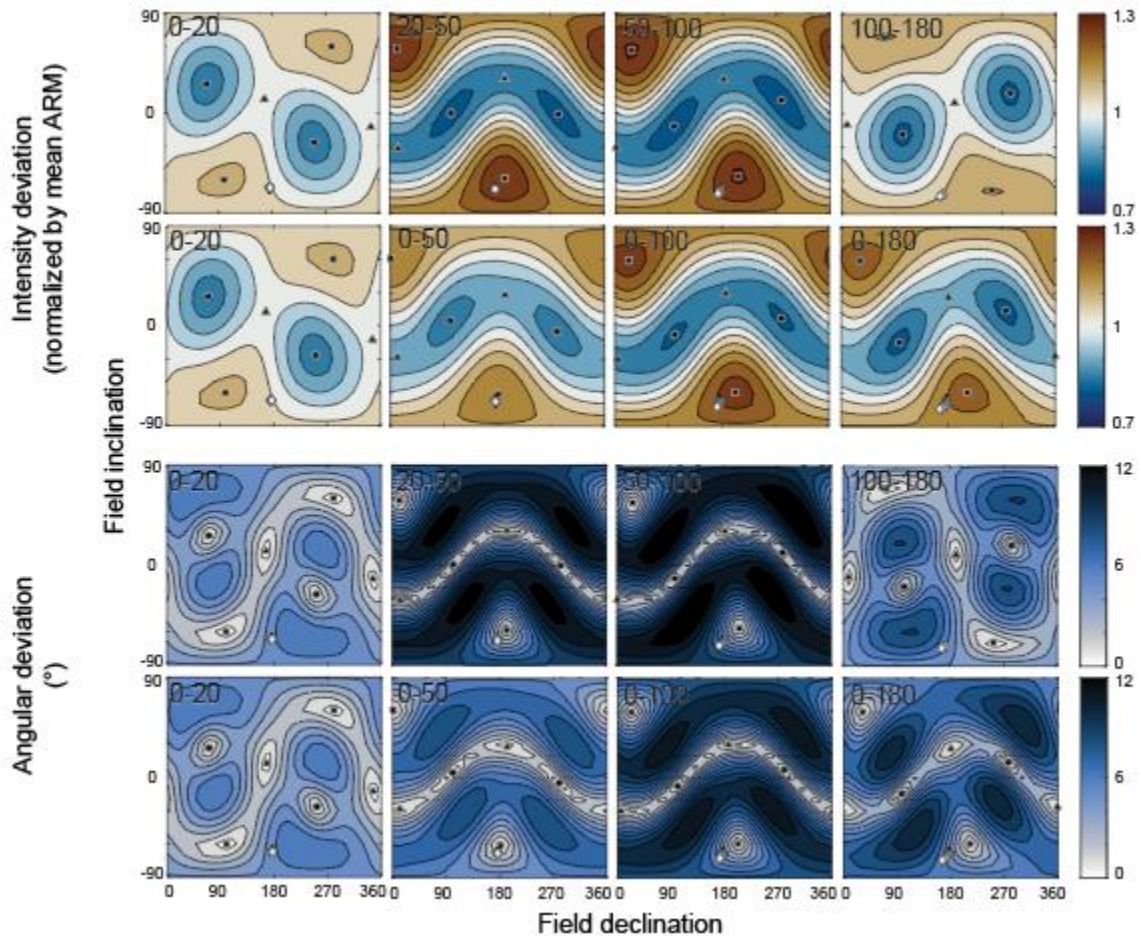
261 To model a natural remanent magnetization (NRM) acquired in constant field conditions, and in the
262 absence of any remagnetization or alteration events, an ARM of known intensity and orientation was
263 applied to each specimen. Successive stepwise demagnetization of this ARM shows that (1) the ARM
264 direction generally deviates from the direction of the applied field, and (2) there appears to be a
265 variation of directions with demagnetization step, resulting in a seemingly two-component
266 magnetization (Figure 5). In a typical paleomagnetic study, the vector endpoint diagrams as shown in
267 Figure 5 would likely be interpreted as 2 components of magnetization acquired at different times.
268 However, in this study the entire magnetization was acquired in a single magnetization event, with a
269 field of constant orientation. Hence, only the coercivity- and grain-size-dependence of the AARM as
270 shown in 4.2 can account for the apparent two-component magnetizations. Similar observations are
271 made during the stepwise acquisition of an ARM in a known field with constant orientation.

272 To determine whether the directions of ARM remaining or acquired in each coercivity window are
273 significantly distinct or share a common mean orientation, they were separated into groups as defined
274 by the AF 0-20 mT (Group 1), 20-50 mT (Group 2), 50-100 mT (Group 3), and 100-200 mT (Group 4)
275 ranges, for both ARM demagnetization and ARM acquisition of each specimen. Note that in doing so,
276 the directions at 20 mT, 50 mT, and 100 mT were each included in two of the sub-groups. Watson's
277 (1983) common mean test was used to assess if the magnetization vectors of two adjacent subgroups
278 have common or different directions (Table 1). Whereas some sub-groups may share a common mean,
279 most subgroups have different mean directions at the 95% confidence limit.



281 *Figure 3: Mean ARM, k' , P , U and principal directions for all ApARM and AARM tensors of each specimen.*
 282 *Blue/black bars are for individual AF windows; pink/tan bars are measured over adjacent windows. Note*
 283 *that the window with the highest mean ARM does not necessarily carry the strongest anisotropy, and*
 284 *that the principal axes, degree and shape of anisotropy can vary dramatically between different*
 285 *A(p)ARMs of the same specimen, and do generally not coincide with the respective parameters for AMS.*

286

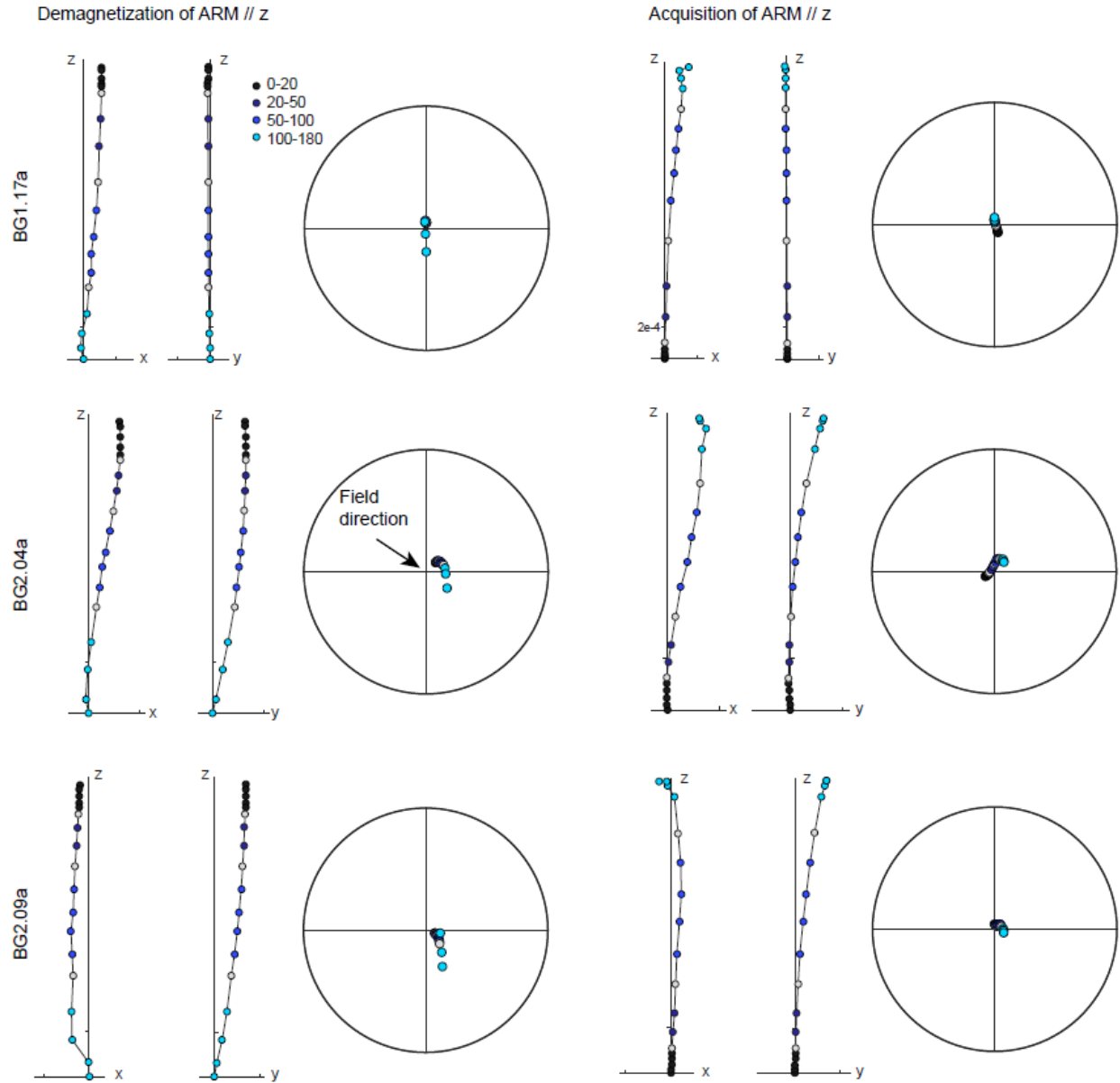


287

288

289 *Figure 4: Angular and intensity deviations for specimen BG2.04a in each coercivity window as compared*
 290 *to an isotropic specimen with the same k_{mean} , magnetized parallel to the field direction, as a function of*
 291 *field declination and field inclination. Squares, triangles, and circles indicate the directions of maximum,*
 292 *intermediate and minimum principal A(p)ARM axes for each window, and diamonds indicate the set of*
 293 *natural remanence directions during AF demagnetization in the same window.*

294



295

296 *Figure 5: Demagnetization of an ARM acquired parallel to z in the lab, and acquisition of an ARM parallel*
 297 *to z. Vector endpoint diagrams with equal axes, and stereonets showing the direction of the ARM after*
 298 *each demagnetization or acquisition step. Tick marks in all vector endpoint diagrams are $2 \cdot 10^{-4} \text{ Am}^2/\text{kg}$.*

299

300

301

302

303

304 *Table 1: Watson (1983) test of common means. 'yes' means that the hypothesis that two subgroups have*
 305 *a common mean cannot be rejected at the 95% confidence interval, 'no' means that the two subgroups*
 306 *have different mean directions at the 95% confidence level*

Sample and group	Demagnetization of ARM // z			Acquisition of ARM // z		
	Watson's V	V critical	Common mean?	Watson's V	V critical	Common mean?
BG1.17a						
Group 1 - Group 2	11.1	7.4	no	1.2	8.8	yes
Group 2 - Group 3	15.9	7.3	no	5.7	8.4	yes
Group 3 - Group 4	0.4	8.9	yes	21.3	7.1	no
Group 4 - Group 1	0.4	8.7	yes	0.5	8.7	yes
BG2.04a						
Group 1 - Group 2	3.3	7.1	yes	13.9	8.2	no
Group 2 - Group 3	7.8	7.2	no	14.8	8.0	no
Group 3 - Group 4	14.2	9.3	no	14.6	7.4	no
Group 4 - Group 1	17.1	9.4	no	369.2	7.0	no
BG2.09a						
Group 1 - Group 2	0.1	7.3	yes	1.1	7.5	yes
Group 2 - Group 3	18.9	7.8	no	11.2	7.3	no
Group 3 - Group 4	13.5	8.9	no	21.6	7.5	no
Group 4 - Group 1	20.2	8.8	no	66.3	7.4	no

307

308 5. Discussion

309 5.1 New protocol for anisotropy corrections

310 Magnetic remanence vectors are commonly corrected for anisotropy using a single AMS, AARM, ATRM
 311 or AIRM tensor, and multiplying the magnetization vector with the inverse of this tensor (adjusted for
 312 single particle anisotropy in the case of depositional remanence) (Jackson et al., 1991; Selkin et al.,
 313 2000). Doing so corrects the overall remanence for the integrated fabric of all remanence-carrying
 314 grains, and works well in rocks with a single remanence carrier which also carries the anisotropy.
 315 However, care has to be taken when several minerals contribute to the remanence and/or anisotropy, in
 316 which case the choice of correct anisotropy tensor is crucial (Bilardello and Kodama, 2010; Selkin et al.,
 317 2000). For this reason, (Selkin et al., 2000) stated that '*paleomagnetists must do more than simply*
 318 *measure AMS to determine whether their specimens are truly affected by remanence anisotropy*'.

319 Ideally, correcting the ARM data as shown in Figure 5 with one adequate remanence anisotropy tensor,
 320 would restore an overall, single-component magnetization parallel to the field. However, in rocks with
 321 multiple remanence carriers and complex fabrics, different subpopulations of grains may form, alter,
 322 and be (re)magnetized at different times. Hence, not all subpopulations of grains will contribute to the
 323 characteristic remanence. Likewise, it is possible that several subpopulations of grains combined carry
 324 the characteristic remanence, but possess different magnetic fabrics, and upon demagnetization of the
 325 NRM it appears as if two (or multiple) components of magnetization are present. No single tensor is able
 326 to correct for a seemingly two-component magnetization, because variations in remanence intensity
 327 and direction related to coercivity-dependent changes in anisotropy will remain unaccounted for. To
 328 account for these effects, we suggest that using a combination of ApARM tensors that reflect the
 329 different subpopulations of grains is a more appropriate basis for anisotropy corrections than using a
 330 single overarching remanence anisotropy tensor. Alternatively, it is possible that the ATRM tensor is

331 much less affected by differing anisotropies in different partial TRMs and use of that tensor would be
332 preferable. However, most of our specimens show signs of alteration or non-ideal behavior in ATRM
333 experiments, and the principal ATRM and ApTRM directions of the one specimen that did pass the
334 alteration test are ill-defined. Therefore, we can neither confirm nor rule out that ApTRMs are different
335 at this stage, and more work will be needed to investigate the variation of ApTRM with blocking
336 temperature.

337 To improve the application of AARM, we propose an updated theory of anisotropic remanence
338 acquisition, which takes into account the dependence of anisotropy on coercivity and grain size. For a
339 rock containing multiple subpopulations of grains (sp1, sp2, ... spn; assume that sp1 contains the fraction
340 of lowest, and spn the fraction of highest coercivities) with distinct magnetic fabrics ($k_{sp1}, k_{sp2} \dots k_{spn}$),
341 the magnetization it acquires in field H is described by $M_{tot} = M_1 + M_2 + \dots + M_n = k_{sp1}H +$
342 $k_{sp2}H + \dots + k_{spn}H$. In the general case when k_{spi} is different for each subpopulation, $M_1, M_2 \dots M_n$,
343 will have different orientations. The anisotropy and remanence of the bulk rock are defined by $k_{tot} =$
344 $k_{sp1} + k_{sp2} + \dots + k_{spn}$, and M_{tot} (Figure 6). In a fully magnetized state, the specimen's
345 magnetization is controlled by all subpopulations of grains together, and thus affected by the
346 combination of all k_{spi} s. During alternating field demagnetization, it is the lowest-coercivity grains that
347 lose their magnetization first, followed by the intermediate and high-coercivity grains. Similarly, in the
348 case of thermal demagnetization, the lowest unblocking temperatures are removed first, although the
349 relationship between coercivity and blocking temperature is not straight forward except for grains
350 whose magnetizations are carried by uniaxial single domain magnetite and we are discussing only the
351 anisotropy of coercivity here. The magnetization is carried by all grains (sp1 ... spn), then sp2 ... spn, sp3
352 ... spn etc., and controlled by the corresponding anisotropies $k_{tot}, k_{sp2} + \dots + k_{spn}, k_{sp3} + \dots + k_{spn}, \dots, k_{spn}$.
353 During ARM acquisition, the lowest-coercivity grains are magnetized first, and the magnetization is
354 affected by k_{sp1} . Subsequently, intermediate and then high-coercivity-grains get magnetized, and their
355 anisotropy also starts contributing to the fabric affecting remanence. Thus, the relevant anisotropy is
356 k_{sp1} , then $k_{sp1}+k_{sp2}, k_{sp1}+k_{sp2}+k_{sp3}, \dots, k_{sp1} + \dots + k_{spn}$. If anisotropy corrections based on these tensors
357 successfully retrieve the field in which the ARM was acquired, both in direction and intensity, they can
358 adequately correct the NRM, provided that ARM is a good proxy for NRM.

359 Using remanence anisotropy applied over a broad coercivity spectrum will activate the remanence-
360 carrying grains only, in contrast to AMS, which describes the fabric of all grains combined. This leads to a
361 more accurate anisotropy correction, because it more closely reflects the fabric of the grains
362 contributing to the remanence. However, in analogy with complex AMS fabrics, where the anisotropy
363 contributions of different minerals can interfere positively or negatively, the remanence anisotropies of
364 sub-populations of grains with different coercivities can also add up or cancel each other out. Therefore,
365 anisotropy corrections should be based on ApARMS rather than AARMS or AMS, to avoid over- or under-
366 correcting the remanence direction and intensity.

367 Measuring ApARMS in finer coercivity windows theoretically leads to more accurate anisotropy
368 corrections; however, care needs to be taken that windows are not too small, resulting in lower signal-
369 to-noise ratios and consequently not significant fabric results. For each specimen, the windows for
370 ApARM characterization should be chosen such that the fabrics of all subpopulations of grains can be
371 isolated (and corrected for), while making sure that the magnetizations measured in each orientation
372 are strong enough to determine reliable anisotropy tensors. We caution that too large windows may

373 lead to under- or over-corrections of parts of the demagnetization curves, whereas coercivity windows
374 that are too small could lead to no significant anisotropy, or to unrealistically high anisotropy when the
375 noise level is higher than the anisotropy.

376 A straightforward test for coercivity-dependent changes in anisotropy is to check for changes in the
377 magnetization directions during an ARM demagnetization or ARM acquisition experiment. The same
378 data can also be used to test if anisotropy corrections are successful, because the field direction and
379 intensity are known. ARM demagnetization or acquisition is routinely measured in paleomagnetic
380 studies in order to verify that ARM is an adequate proxy for NRM. For this, the intensity of ARM is
381 compared to that of the NRM during NRM demagnetization. Because the ARM direction is measured as
382 a by-product, these data can be used as a first estimate of anisotropy and changes in anisotropy, by
383 checking (1) whether the ARM is parallel to the field in which it was acquired, and (2) how the ARM
384 direction varies with coercivity. If an ARM is not parallel to the field, this indicates anisotropy, and if its
385 direction varies systematically throughout the ARM demagnetization or ARM acquisition, then this can
386 be related to changes in remanence anisotropy with coercivity. Note that, if the field is applied parallel
387 to one of the principal remanence susceptibility directions, the ARM is parallel to the field even in
388 presence of anisotropy. In this case, ARM anisotropy can still be detected if the ARM is imparted along
389 several directions, e.g. x, y, and z, because the intensities will be different. Similarly, the direction of
390 laboratory pTRM acquired in paleointensity experiments can be monitored (as is done in the Thellier GUI
391 program of Shaar and Tauxe (2013)) and checked for anisotropy as well as anisotropy variations with
392 temperature.

393 5.2 Anisotropy corrections for our specimens

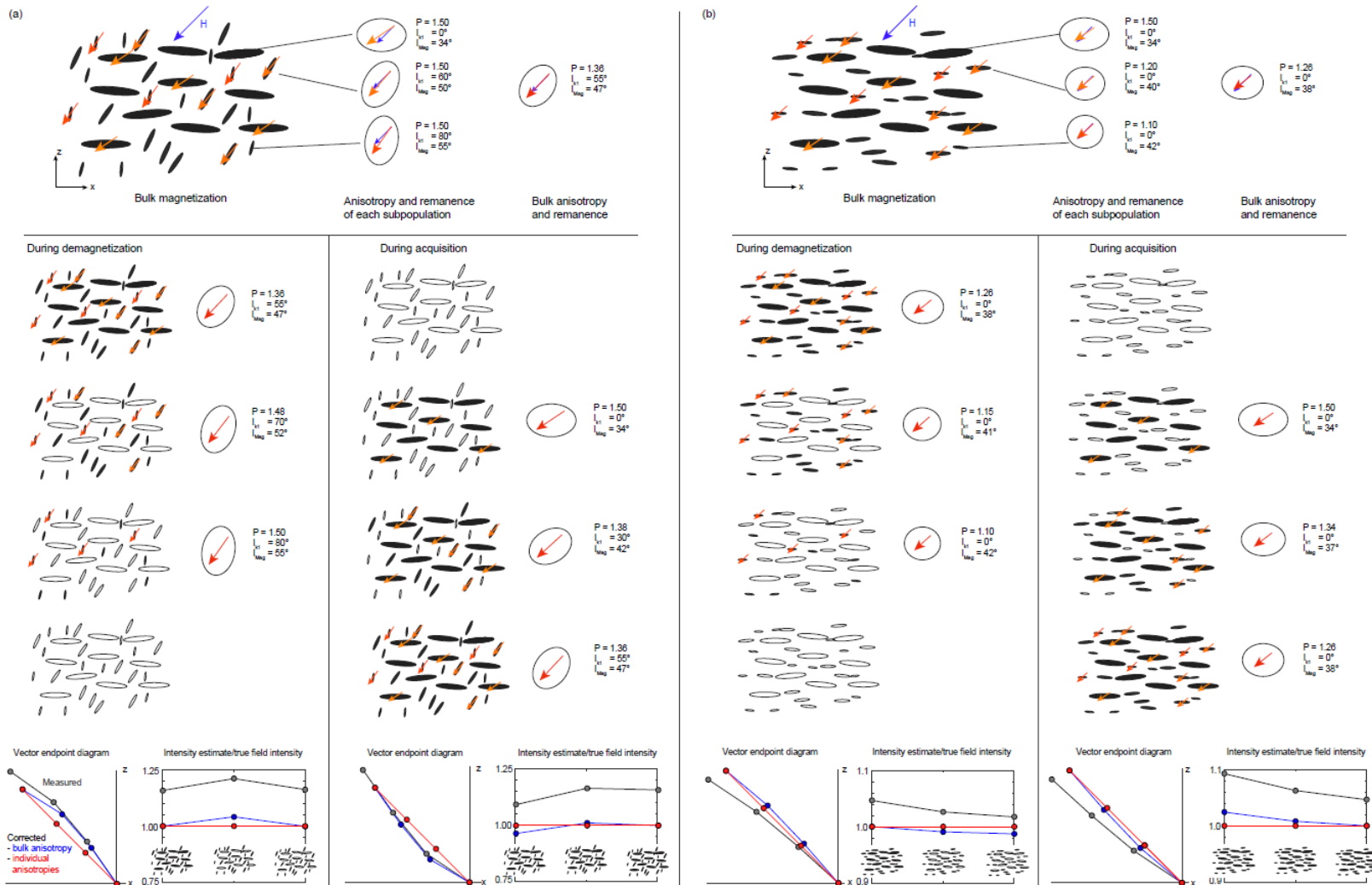
394 The differences in ApARM tensors indicates that our specimens comprise several subpopulations of
395 remanence carriers, each with a different fabric. Other than for the synthetic model, it is not known *a*
396 *priori* how many subpopulations there are, which coercivity windows they correspond to, or whether
397 the coercivity windows of two (or several) subpopulations overlap. Further, there were more
398 demagnetization steps in the ARM demagnetization or acquisition experiments than there were
399 coercivity windows for the ApARM measurements. ApARMs were measured for coercivity windows of 0-
400 20, 20-50, 50-100 and 100-180 mT. ARM demagnetization and ARM acquisition was measured in fields
401 of 2, 5, 10, 15, 20, 30, 40, 50, 60, 70, 80, 90, 100, 120, 140, 160, 180, 200 mT on the DTech/2G, and 2, 5,
402 10, 15, 20, 30, 40, 50, 60, 70, 80, 90, 100, 120, 140, 160, 170 mT on the u-channel. For the
403 demagnetization or acquisition steps at 0, 20, 50, 100 and 180 mT, the combination of ApARMs affecting
404 the remanence and that should be used for the anisotropy correction, corresponds to the findings of the
405 synthetic model. However, for all other steps, it is more complicated. For example, the demagnetization
406 step at 30 mT is affected partly by the ApARM in the 20-50 mT window, as well as the anisotropies
407 carried by higher-coercivity grains, as measured by the ApARMs in higher coercivity windows. This can
408 be expressed as $a \cdot k_{20-50} + k_{50-100} + k_{100-180}$. Conversely, during acquisition of ARM, the magnetization at 30
409 mT is affected by the remanence anisotropies of all windows with lower coercivities, as well as the
410 window comprising the 30 mT step; $k_{0-20} + b \cdot k_{20-50}$. The coefficients *a* and *b* can be approximated by the
411 ratio $k_{mean_{30-50}}/k_{mean_{20-50}}$, and $k_{mean_{20-30}}/k_{mean_{20-50}}$, i.e. $a = 1-b$. Assuming that the mean ARM decay
412 or gain is linear in each window, *a* and *b* can also be estimated from the fields at which the
413 magnetization is measured, i.e. $a = (50-30)/(50-20)$ and $b = (30-20)/(50-20)$.

414 Synthetic ‘paleo’ directions and ‘paleo’ intensities were computed from the magnetizations during the
 415 demagnetization/acquisition of ARM experiments using different types of anisotropy corrections: (1)
 416 isotropic correction with mean ARM susceptibility, (2) anisotropy correction with the AARM₀₋₁₀₀ tensor,
 417 (3) anisotropy correction with the AARM₀₋₁₈₀ tensor, (4) anisotropy correction based on ApARM₀₋₂₀,
 418 ApARM₂₀₋₅₀, ApARM₅₀₋₁₀₀ and ApARM₁₀₀₋₁₈₀, correcting all the measurements between 0-20 mT AF for
 419 ApARM₂₀₋₁₈₀, between 20-50 mT AF for ApARM₅₀₋₁₈₀, etc., and (5) anisotropy correction based on
 420 ApARM₀₋₂₀, ApARM₂₀₋₅₀, ApARM₅₀₋₁₀₀ and ApARM₁₀₀₋₁₈₀, correcting the measurements between 0-20 mT
 421 AF for the interpolated ApARM₂₀₋₁₈₀ + α *ApARM₀₋₂₀, etc. Figure 7 shows vector endpoint diagrams for the
 422 demagnetization and acquisition of an ARM parallel to the specimen z-axis before and after correction.

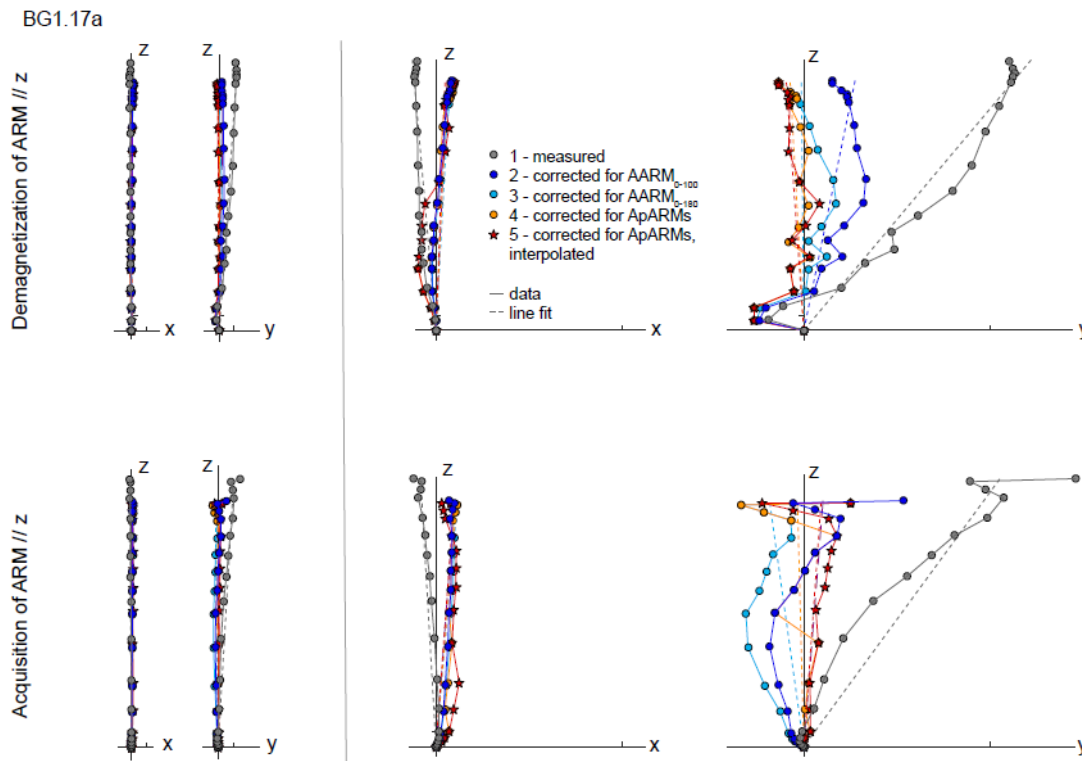
423 The quality of each correction was assessed by comparing (1) the estimated directions of measured
 424 magnetization as well as directions of best-fit lines, and (2) intensities with the known direction and
 425 intensity of the field (Figure 8). For directions, the measures $\sqrt{M_x^2 + M_y^2}$, and
 426 $\sqrt{(M_x^2 + M_y^2)/(M_x^2 + M_y^2 + M_z^2)}$ describe how much the measured magnetization deviates from
 427 the direction of the field for each specimen and each type of correction. $\sqrt{M_x^2 + M_y^2}$ decreases by
 428 about a factor of 2 when anisotropic corrections (2) – (5) are used compared to the mean ARM. In
 429 general, there is a slight decrease in $\sqrt{M_x^2 + M_y^2}$ from (2) and (3) to (4) and (5), however, this is small
 430 compared to the difference between isotropic and (any) anisotropic correction. While the measure
 431 $\sqrt{(M_x^2 + M_y^2)/(M_x^2 + M_y^2 + M_z^2)}$ generally decreases when anisotropy-corrected, it may be larger
 432 after correction with AARM₀₋₁₈₀ than for the isotropic correction. This indicates that for some specimens,
 433 anisotropy corrections based on an overall AARM may result in worse estimates of the paleofield
 434 direction than if the data was not corrected. Many specimens show little variation between the
 435 corrections (2), (3) and (4), however, for some $\sqrt{(M_x^2 + M_y^2)/(M_x^2 + M_y^2 + M_z^2)}$ markedly decreases
 436 from (2)/(3) to (4)/(5). Similar observations can be made based on the inclination of the best-fit lines
 437 with respect to field direction. Hence, whereas the type of correction may not have much influence on
 438 the estimated field direction for the majority of specimens, for some specimens determining individual
 439 ApARMs and adding parts of all ApARMs that may contribute significantly improves anisotropy
 440 corrections as compared to the integrated AARM₀₋₁₀₀ or AARM₀₋₁₈₀.

441 The reliability of intensity estimates was characterized by the ratio of estimated intensity and known
 442 field intensity, for the ARM at fields 0, 20, 50, 100 and 180 mT AF. Hence, only corrections (1) – (4) were
 443 calculated. The ratio is generally closer to 1 for corrections (2) – (4) than the isotropic correction (1).
 444 Similar as for the estimate of directions, the changes between (2)/(3) and (4) are generally small, but for
 445 some specimens, the bulk AARM corrections (2) or (3) result in larger deviations from the known
 446 intensity than the uncorrected data, or after correction with individual tensors. Hence, the error in
 447 estimated intensity may increase for an anisotropy correction based on a bulk AARM as compared to a
 448 paleointensity estimate assuming the specimen is isotropic. For these specimens, the accuracy of
 449 intensity estimates significantly increases when the anisotropy corrections are based on a set of
 450 individual ApARMs. Note that intensity estimates can additionally be affected by decay rate effects, if

451 the A(p)ARM and ARM demagnetization/acquisition experiments were performed on different
452 instruments (cf. Figure A, online supplementary for a thorough discussion of this effect).



455 *Figure 6: Conceptual model of remanence acquisition and demagnetization in a rock with several subpopulations of grains with different*
 456 *anisotropies. Filled grains are magnetized, open grains are demagnetized. (a) shows the effect of variations in fabric orientation with constant*
 457 *degree of anisotropy, and (b) shows the effect of variations in anisotropy degree with constant fabric orientation. H indicates magnetizing field.*



459

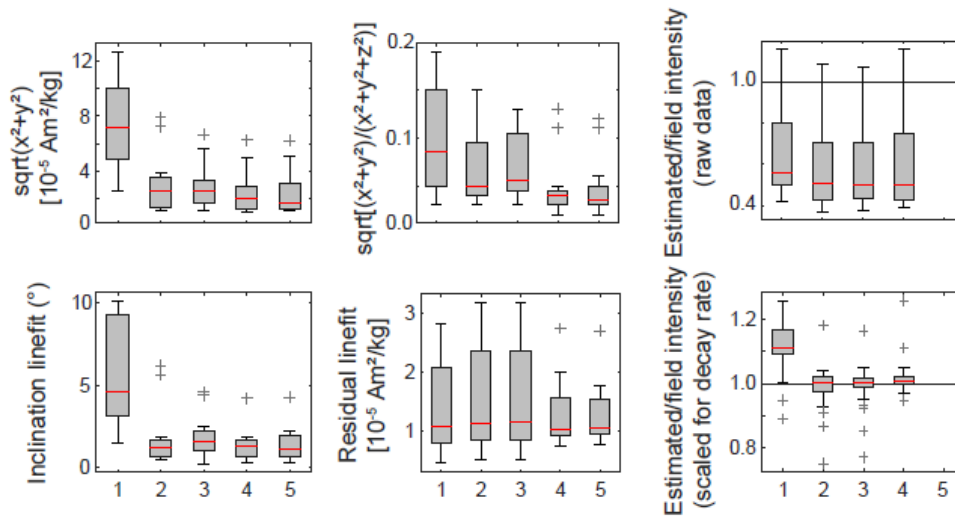
460 *Figure 7: Vector endpoint diagrams for BG1.17a for demagnetization and acquisition of an ARM parallel*
 461 *to z as measured, and after different types of anisotropy corrections. Vector endpoint diagrams are*
 462 *shown with equal axes (left) and an expanded horizontal axis (right), and tick marks indicate a*
 463 *magnetization of $1 \cdot 10^{-4} \text{ Am}^2/\text{kg}$.*

464

465 5.3 Implications for anisotropy corrections in future studies

466 The results presented here suggest that for rocks with complex remanence anisotropies, it may be
 467 necessary to use anisotropy corrections based on a combination of ApARMs rather than a single AARM
 468 tensor. More work will be needed to determine whether the same is true for ATRMs, or if anisotropy of
 469 TRM behaves differently. By analogy, it is possible that ATRM varies with the temperature interval over
 470 which TRMs are imparted. Future studies should investigate this effect, and relate the temperature-
 471 dependence of ATRM to the direction of pTRMs acquired in paleointensity studies. A potential challenge
 472 with this type of investigation is that each heating step increases the risk of specimen alteration.

473 Whether or not these more advanced ARM anisotropy corrections are needed depends on the
 474 remanence carriers and their fabrics, particularly the interplay of their individual anisotropies. In
 475 specimens with a single remanence carrier and a single fabric, remanence anisotropy likely does not
 476 depend on coercivity, and therefore a simple correction may be sufficient. On the contrary, in rocks with
 477 multiple remanence carriers and complex fabrics, the interplay of individual anisotropies may call for a
 478 more advanced anisotropy correction. Coercivity-dependent changes in remanence anisotropy should
 479 be checked for on all rocks with complex fabrics of remanence-carrying minerals, because it is not clear
 480 a priori how the individual fabrics interact and if a more advanced anisotropy correction is necessary.



482

483 *Figure 8: Error in direction and intensity after different anisotropy corrections. (1) isotropic correction*
 484 *with mean ARM susceptibility, (2) anisotropy correction with the $AARM_{0-100}$ tensor, (3) anisotropy*
 485 *correction with the $AARM_{0-180}$ tensor, (4) anisotropy correction based on $ApARM_{0-20}$, $ApARM_{20-50}$,*
 486 *$ApARM_{50-100}$ and $ApARM_{100-180}$, correcting all the measurements between 0-20 mT AF for $ApARM_{20-180}$,*
 487 *between 20-50 mT AF for $ApARM_{50-180}$, etc., and (5) interpolated anisotropy correction based on $ApARM_{0-20}$,*
 488 *$ApARM_{20-50}$, $ApARM_{50-100}$ and $ApARM_{100-180}$, correcting the measurements between 0-20 mT AF for*
 489 *$ApARM_{20-180} + \alpha * ApARM_{0-20}$, etc. The reader is referred to the online supplementary for a discussion on*
 490 *the effect of decay rates on the intensity estimates. Boxplots include ARM demagnetization and ARM*
 491 *acquisition for 8 specimens and 19 steps each for directions, and demagnetization and acquisition for 8*
 492 *specimens and 4 steps for intensities*

493

494 6. Conclusions and suggestions for future studies

495 Remanence anisotropy affects both the direction and intensity of magnetization, and may need to be
 496 corrected for in paleomagnetic and paleointensity studies. Previous work has highlighted the
 497 importance of isolating the anisotropy of the remanence-carrying grains prior to anisotropy corrections,
 498 when anisotropy and remanence are carried by different minerals (Bilardello and Kodama, 2010; Selkin
 499 et al., 2000). Here, we expand these findings to rocks with multiple remanence and anisotropy carriers,
 500 and illustrate how grain-size dependent anisotropies and fabrics affect magnetization. When A(p)ARM
 501 varies with coercivity or grain size, this variation can lead to a seemingly multi-component
 502 magnetization, even if a specimen is magnetized in a single event and constant field. This study further
 503 shows how anisotropy corrections can be adapted in rocks with multiple remanence carriers with
 504 distinct fabrics. We suggest that these procedures are applied in future studies, rather than the
 505 traditional correction for the bulk anisotropy in a specimen, if specimens contain multiple remanence
 506 carriers with different fabrics. More work will be needed to determine whether similar effects are
 507 observed for A(p)TRMs acquired over different temperature intervals.

508 A simple initial test whether remanence anisotropy is coercivity dependent can be done based on
509 directions of ARM imparted in a known field. This test is convenient because ARM acquisition or ARM
510 demagnetization are measured anyway in paleomagnetic studies. Systematic changes in ARM direction
511 with AF step indicate changes in remanence anisotropy. A more complete assessment can be reached by
512 determining ApARMs for different coercivity windows.

513 Finally, the results presented here indicate that AARM tensors and hence anisotropy corrections are
514 dependent on the experimental parameters that were used when the remanence anisotropy was
515 measured. In addition to the coercivity-dependence, we find a strong variation between mean ARMs
516 acquired on different instruments. We therefore encourage researchers to report all experimental
517 parameters, particularly coercivity window and decay rate that were used to impose ARMs, in future
518 studies.

519 Acknowledgments

520 This project was funded by the Swiss National Science Foundation (SNSF), project 167608. The IRM is a
521 US National Multi-user Facility supported through the Instrumentation and Facilities program of the
522 National Science Foundation, Earth Sciences Division, and by funding from the University of Minnesota.
523 Collection of the specimens from the Bushveld Complex was supported by NSF-EAR 0309686 awarded to
524 Paul Renne and Gary Scott. LT acknowledges support from the National Science Foundation under Grant
525 No. 1547263. This is IRM publication #1802. Data can be obtained from the Supplementary Material of
526 this paper, or downloaded from the MagIC database, doi:xxxxxxx.

527 References

- 528 Aubourg, C., Robion, P., 2002. Composite ferromagnetic fabrics (magnetite, greigite) measured by AMS
529 and partial AARM in weakly strained sandstones from western Makran, Iran. *Geophysical Journal*
530 *International* 151, 729-737.
- 531 Ben-Yosef, E., Tauxe, L., Levy, T.E., 2010. Archaeomagnetic dating of copper smelting site F2 in the Timna
532 Valley (Israel) and its implications for the modelling of ancient technological developments.
533 *Archaeometry* 52, 1110-1121.
- 534 Biggin, A.J., Piispa, E.J., Pesonen, L.J., Holme, R., Paterson, G.A., Veikkolainen, T., Tauxe, L., 2015.
535 Palaeomagnetic field intensity variations suggest Mesoproterozoic inner-core nucleation. *Nature*
536 526, 245-248.
- 537 Biggin, A.J., Steinberger, B., Aubert, J., Suttie, N., Holme, R., Torsvik, T.H., van der Meer, D.G., van
538 Hinsbergen, D.J.J., 2012. Possible links between long-term geomagnetic variations and whole-mantle
539 convection processes. *Nature Geoscience* 5, 526-533.
- 540 Bilardello, D., Jackson, M.J., 2014. A comparative study of magnetic anisotropy measurement techniques
541 in relation to rock-magnetic properties. *Tectonophysics* 629, 39-54.
- 542 Bilardello, D., Kodama, K.P., 2010. A new inclination shallowing correction of the Mauch Chunk
543 Formation of Pennsylvania, based on high-field AIR results: Implications for the Carboniferous North
544 American APW path and Pangea reconstructions. *Earth and Planetary Science Letters* 299, 218-227.
- 545 Borradaile, G.J., Almqvist, B.S., 2008. Correcting distorted paleosecular variation in late glacial lacustrine
546 clay. *Physics of the Earth and Planetary Interiors* 166, 30-43.
- 547 Borradaile, G.J., Lacroix, F., Trimble, D., 2001. Improved isolation of archeomagnetic signals by combined
548 low temperature and alternating field demagnetization. *Geophysical Journal International* 147, 176-
549 182.

550 Bowles, J., Gee, J.S., Kent, D.V., Bergmanis, E., Sinton, J., 2005. Cooling rate effects on paleointensity
551 estimates in submarine basaltic glass and implications for dating young flows. *Geochemistry,*
552 *Geophysics, Geosystems* 6, Q07002.

553 Buffett, B.A., 2003. The thermal state of Earth's core. *Science* 299, 1675-1677.

554 Cisowski, S.M., Collinson, D.W., Runcorn, S.K., Stephenson, A., Fuller, M., 1983. A review of lunar
555 paleointensity data and implications for the origin of lunar magnetism. *Journal of Geophysical*
556 *Research - Solid Earth* 88, A691-A704.

557 Coe, R.S., 1967. The determination of paleo-intensities of the Earth's magnetic field with emphasis on
558 mechanisms with could cause non-ideal behavior in Thellier's method. *Journal of Geomagnetism*
559 *and Geoelectricity* 19, 157-179.

560 Cottrell, R.D., Tarduno, J.A., 1999. Geomagnetic paleointensity derived from single plagioclase crystals.
561 *Earth and Planetary Science Letters* 169, 1-5.

562 Dietz, R.S., Holden, J.C., 1970. Reconstruction of Pangea: Breakup and dispersion of continents, Permian
563 to Present. *Journal of Geophysical Research* 75, 4939-4956.

564 Dunlop, D.J., Schmidt, P.W., Özdemir, Ö., Clark, D.A., 1997. Paleomagnetism and paleothermometry of
565 the Sydney Basin, 1, Thermoviscous and chemical overprinting of the Milton Monzonite. *Journal of*
566 *Geophysical Research*, 102, 27285-27295.

567 Elmore, R.D., Muxworthy, A.R., Aldana, M., 2012. Remagnetization and chemical alteration of
568 sedimentary rocks. In: Elmore, R.D., Muxworthy, A.R., Aldana, M.M., Mena, M. (eds) 2012.
569 Remagnetization and chemical alteration of sedimentary rocks, Geological Society, London, Special
570 Publications, 371, doi: 10.1144/SP371.15.

571 Evans, M.E., 1976. Test of the dipolar nature of the geomagnetic field throughout Phanerozoic time.
572 *Nature* 262, 676-677.

573 Feinberg, J.M., Scott, G.R., Renne, P.R., Wenk, H.-R., 2005. Exsolved magnetite inclusions in silicates:
574 Features determining their remanence behavior. *Geology* 33, 513.

575 Feinberg, J.M., Wenk, H.-R., Scott, G.R., Renne, P.R., 2006. Preferred orientation and anisotropy of
576 seismic and magnetic properties in gabbro-norites from the Bushveld layered intrusion.
577 *Tectonophysics* 420, 345-356.

578 Gattacceca, J., Rochette, P., Bourot-Denise, M., 2003. Magnetic properties of a freshly fallen LL ordinary
579 chondrite: the Bensour meteorite. *Physics of the Earth and Planetary Interiors* 140, 343-358.

580 Hale, C.J., 1987. Palaeomagnetic data suggest link between the Archaean-Proterozoic boundary and
581 inner-core nucleation. *Nature* 329, 233-237.

582 Hattingh, P.J., 1986. The palaeomagnetism of the Main Zone in the western Bushveld Complex. *Earth*
583 *and Planetary Science Letters* 79, 441-452.

584 Hext, G. R., 1963. The estimation of second-order tensors, with related tests and designs. *Biometrika*
585 50(3/4), 353-373.

586 Hospers, J., van Andel, S.I., 1969. Palaeomagnetism and tectonics: a review. *Earth-Science Reviews* 5, 5-
587 44.

588 Irving, E., 1957. Rock magnetism: A new approach to some palaeogeographic problems. *Advances in*
589 *Physics* 6, 194-218.

590 Jackson, M., Gruber, W., Marvin, J., Banerjee, S.K., 1988. Partial anhysteretic remanence and its
591 anisotropy: applications and grain-size-dependence. *Geophysical Research Letters* 15, 440-443.

592 Jackson, M.J., Banerjee, S.K., Marvin, J.A., Lu, R., Gruber, W., 1991. Detrital remanence, inclination
593 errors, and anhysteretic remanence anisotropy: quantitative model and experimental results.
594 *Geophysical Journal International* 104, 95-103.

595 Kent, D.V., Irving, E., 2010. Influence of inclination error in sedimentary rocks on the Triassic and Jurassic
596 apparent pole wander path for North America and implications for Cordilleran tectonics. *Journal of*
597 *Geophysical Research - Solid Earth* 115.

598 Kodama, K.P., Dekkers, M.J., 2004. Magnetic anisotropy as an aid to identifying CRM and DRM in red
599 sedimentary rocks. *Studia Geophysica Et Geodaetica* 48, 747-766.

600 Letts, S., Torsvik, T.H., Webb, S.J., Ashwal, L.D., 2009. Palaeomagnetism of the 2054 Ma Bushveld
601 Complex (South Africa): Implications for emplacement and cooling. *Geophysical Journal
602 International* 179, 850-872.

603 Levi, S., 1977. The effect of magnetite particle size on paleointensity determinations of the geomagnetic
604 field. *Physics of the Earth and Planetary Interiors* 13, 245-259.

605 Mitra, R., Tauxe, L., McIntosh, S.K., 2013. Two thousand years of archeointensity from West Africa. *Earth
606 and Planetary Science Letters* 364, 123-133.

607 Morel, P., Irving, E., 1981. Paleomagnetism and the evolution of Pangea. *Journal of Geophysical
608 Research - Solid Earth* 86, 1858-1872.

609 Pesonen, L.J., Nevanlinna, H., 1981. Late Precambrian Keweenawan asymmetric reversals. *Nature* 294,
610 436-439.

611 Potter, D.K., 2004. A comparison of anisotropy of magnetic remanence methods - a user's guide for
612 application to paleomagnetism and magnetic fabric studies, in: Martín-Hernández, F., Lüneburg,
613 C.M., Aubourg, C., Jackson, M. (Eds.), *Magnetic Fabrics: Methods and Applications*. The Geological
614 Society, London, UK, pp. 21-35.

615 Prévot, M., Mankinen, E.A., Coe, R.S., Grommé, C.S., 1985. The Steens Mountain (Oregon) geomagnetic
616 polarity transition: 2. Field intensity variations and discussion of reversal models. *Journal of
617 Geophysical Research - Solid Earth* 90, 10417-10448.

618 Rogers, J., Fox, J. M. W., Aitken, M.J., 1979. Magnetic anisotropy in ancient pottery, *Nature* 277(5698),
619 644-646.

620 Selkin, P.A., Gee, J.S., Tauxe, L., 2007. Nonlinear thermoremanence acquisition and implications for
621 paleointensity data. *Earth and Planetary Science Letters* 256, 81-89.

622 Selkin, P.A., Gee, J.S., Tauxe, L., Meurer, W.P., Newell, A.J., 2000. The effect of remanence anisotropy on
623 paleointensity estimates: a case study from the Archean Stillwater Complex. *Earth and Planetary
624 Science Letters* 183, 403-416.

625 Selkin, P. A., Gee, J.S., Meurer, W.P., Hemming, S.R., 2008. Paleointensity record from the 2.7 Ga
626 Stillwater Complex, MT, *Geochemistry Geophysics Geosystems* 9, Q12023,
627 doi:10.1029/2008GC001950.

628 Shaar, R. and Tauxe, L., 2013. Thellier GUI: An integrated tool for analyzing paleointensity data from
629 Thellier-type experiments, *Geochemistry, Geophysics, Geosystems*, 14, doi:10.1002/ggge.20062.

630 Smirnov, A.V., Kulakov, E.V., Foucher, M.S., Bristol, K.E., 2017. Intrinsic paleointensity bias and the long-
631 term history of the geodynamo. *Science Advances* 3, e1602306.

632 Stillinger, M.D., Hardin, J.W., Feinberg, J.M., Blakely, J.A., 2016. Archaeomagnetism as a complementary
633 dating technique to address the Iron Age chronology debate in the Levant. *Near Eastern
634 Archaeology* 79, 90-106.

635 Swanson-Hysell, N.L., Maloof, A.C., Weiss, B.P., Evans, D.A.D., 2009. No asymmetry in geomagnetic
636 reversals recorded by 1.1-billion-year-old Keweenawan basalts. *Nature Geoscience* 2, 713-717.

637 Tarduno, J.A., Cottrell, R.D., Smirnov, A.V., 2006. The paleomagnetism of single crystals: Recording
638 geomagnetic field strength during mixed polarity intervals, superchrons, and inner core growth.
639 *Reviews of Geophysics* 44.

640 Tauxe, L., Kent, D.V., 2004. A simplified statistical model for the geomagnetic field and the detection of
641 shallow bias in paleomagnetic inclinations: was the ancient magnetic field dipolar? *Geophysical
642 Monograph Series* 145.

643 Tauxe, L., Pick, T., Kok, Y.S., 1995. Relative paleointensity in sediments: a pseudo-Thellier approach.
644 *Geophysical Research Letters* 22, 2885-2888.

645 Tauxe L., Yamazaki T., 2015. Paleointensities. In: Gerald Schubert (editor-in-chief) Treatise on
646 Geophysics, 2nd edition, Vol 5. Oxford: Elsevier; p. 461-509.

647 Tema, E., 2009. Estimate of the magnetic anisotropy effect on the archaeomagnetic inclination of
648 ancient bricks. *Physics of the Earth and Planetary Interiors* 176, 213-223.

649 Trindade, R.I.F., Raposo, M.I.B., Ernesto, M., Siqueira, R., 1999. Magnetic susceptibility and partial
650 anhysteretic remanence anisotropies in the magnetite-bearing granite pluton of Tourao, NE Brazil.
651 *Tectonophysics* 314, 443-468.

652 van der Voo, R., Torsvik, T.H., 2001. Evidence for late Paleozoic and Mesozoic non-dipole fields provides
653 and explanation for the Pangea reconstruction problems. *Earth and Planetary Science Letters* 187,
654 71-81.

655 Walton, D., 1980. Time-temperature relations in the magnetization of assemblies of single domain
656 grains. *Nature* 286, 245-247.

657 Watson, G.S., 1983. Large sample theory of the Langevin distribution. *Journal of Statistical Planning and*
658 *Inference* 8, 245-256.

659 Yu, Y., 2011. Importance of cooling rate dependence of thermoremanence in paleointensity
660 determination. *Journal of Geophysical Research*, 116, B09101, doi: 10.1029/2011JB008388.

661 Yu, Y., Tauxe, L., Genevey, A., 2004. Toward an optimal geomagnetic field intensity determination
662 technique. *Geochemistry, Geophysics, Geosystems* 5, Q02H07, doi:10.1029/2003GC000630.

663

664 *Table A: Summary of TRM anisotropy parameters for BG2.09a:*

665 *Table B: Summary of the ranges in mean (p)ARM, normalized eigenvalues, and A(p)ARM parameters for*
666 *each coercivity window across all specimens:*

667 *Table C: Anisotropy of anhysteretic and partial anhysteretic remanence:*

668